JOURNAL OF GEOPHYSICAL RESEARCH, VOL. 101, NO. C9, PAGES 20,799–20,808, SEPTEMBER 15, 1996

Polar boundary layer plumes and bottom water formation: A missing element in ocean general circulation models

L.D. Danny Harvey
Department of Geography, University of Toronto, Toronto, Ontario, Canada

Abstract. Much of the deep water in the world oceans forms as relatively dense water on shelves in polar regions, followed by downslope flow of the dense water as a boundary layer plume. This process is omitted from current global ocean general circulation models (GCMs) which, instead, form bottom water only as a result of the large-scale thermohaline overturning and as a result of deep convection. Here the role of polar boundary layer plumes is investigated by coupling a two-dimensional plume model to a two-dimensional (latitude-depth) dynamical ocean model, which, in turn, is coupled to sea ice and surface climate models. The polar plume mass flux at the shelf brink is parameterized in terms of the rate of sea ice formation, net evaporation, and surface cooling over polar shelves. The presence of plumes has only a modest impact on the high-latitude temperature response to a greenhouse gas increase and the projected sea level rise due to thermal expansion because, in the present model, the overall response is strongly conditioned by changes in the relative strength of northern hemisphere and southern hemisphere bottom waters which occur whether or not plumes are included. These changes, in turn, appear to depend critically on the spin-up flow field and density fields produced by the coupled model. It is concluded that polar plume processes should be incorporated in coupled atmosphere-ocean GCMs but that correct simulation of the ocean density field and surface forcing conditions is a more important priority.

Introduction

Deep or bottom water is formed in current ocean general circulation models (GCMs) by two processes: through convective overturning and mixing when the water column becomes vertically unstable and through deep thermohaline overturning. These two processes are distinct, in that the former depends on the vertical density gradient while the latter depends on the horizontal density gradient, but they are sometimes used interchangeably in the oceanographic literature as if they were the same thing. Convective overturning homogenizes the water column in the depth interval within which it occurs and, in some regions, can extend to the local ocean floor, thereby conditioning the properties of bottom water which may then spread laterally, but such lateral spreading is dependent on horizontal density contrasts and forms part of the thermohaline circulation. Convective overturning will influence the thermohaline circulation only to the extent that it affects horizontal density differences by changing water properties at depth in one region but not in others.

There is, however, a third process by which bottom water is formed in the oceans but which has not yet been incorporated in any global scale ocean GCM. This process is the formation of relatively dense water on shelves in the Weddell Sea and Greenland/Norwegian/Iceland Sea regions, followed by downslope flow of the dense water mass as a boundary layer plume. A number of one-dimensional and two-dimensional plume models have been constructed to model this process [*Smith*, 1975; *Killworth*, 1975, 1977], but no such model has yet been coupled to an ocean GCM. Dense water is formed in the Weddell Sea through brine ejection due to seasonal sea ice formation and its mixing with water from the off-shelf pycnocline, forming Antarctic Bottom Water (AABW). In contrast, dense water forms in the North Atlantic primarily through seasonal cooling of relatively salty and hence relatively dense surface water, without sea ice formation, and flows through passages between Greenland-Iceland and Iceland-Scotland to form North Atlantic Deep Water (NADW). The driving force behind the sinking of such water is the local density difference between the plume and adjacent water, in contrast to the larger scale horizontal density difference which drives the thermohaline overturning outside the bottom boundary layer. Numerous studies have shown that the deep thermohaline circulation in model oceans is highly sensitive to seemingly minor changes in the treatment of surface boundary conditions [i.e., *Huang*, 1993], convective mixing [*Marotzke*, 1991], or ocean bathymetry [*Moore and Reason*, 1993]. The incorporation of boundary layer plumes with fluxes comparable to those simulated for the large scale thermohaline overturning could therefore have a significant effect on the flow field and its interannual variability, as simulated by ocean models for the present climate.

The inclusion of polar boundary layer plumes in GCMs might also affect the model response to surface warming associated with greenhouse gas increases. Where the ocean mixed layer is largely covered by sea ice for both the

Paper number 96JC01796.
0148-0227/96/96JC-01796$09.00

present climate and in a future, warmer climate, little to no warming will occur. In contrast, regions free of sea ice are free to warm as the overall climate warms. To the extent that the source waters for plumes that sink to the ocean bottom are tied to sea ice freezing, warming of the plumes will be suppressed relative to the global mean surface warming as long as sea ice persists. This, in turn, will tend to limit deep ocean warming and associated sea level rise compared to the case in which plumes are not represented. A consistent result obtained by both two-dimensional and three-dimensional ocean models is a transient weakening of thermohaline overturning when the climate warms but a strengthening of the thermohaline circulation in the new steady state [see *Harvey*, 1994]. In some cases, more dramatic transient ocean circulation changes can occur, with significant effects on the transient surface temperature response [*Harvey*, 1994]. Given that a significant fraction of bottom water is formed as boundary layer plumes tied in part to seasonal sea ice processes, both the transient and steady state response to warming could be different from the case in which plumes are not included. Thus there are reasons for expecting that the incorporation of polar boundary layer plumes in ocean GCMs, as found in the real world, will affect the model thermal, dynamical, and sea level response to global warming, with potentially important feedbacks on the rate and magnitude of surface temperature warming.

The purpose of this paper is, first, to draw attention to the fact that a potentially important process has been entirely omitted from the current generation of ocean GCMs and, second, to investigate the potential importance of polar boundary layer plumes to the transient and steady state response to greenhouse gas increases by coupling a simple plume model to a two-dimensional ocean model, which, in turn, is coupled to an energy balance surface climate model and sea ice model. In the next section, pertinent observations of the polar boundary layer plumes are briefly summarized. This is followed by a description of the plume model adopted here and, finally, results of sensitivity tests.

Observations of Polar Plumes

Antarctic Region

AABW is formed primarily in the Weddell Sea and, to a lesser extent, in the Ross Sea and off the Adelie coast. *Gill* [1973], *Carmack and Foster* [1975], *Foster and Middleton* [1980], *Foster et al.* [1987], *Foldvik and Gammelsrod* [1988], and *Gordon et al.* [1993], among others, discuss the process of AABW formation in the Weddell Sea. Dense, cold, and salty water forms on the Weddell Sea shelf (depth, 400-500 m) due to brine rejection associated with net sea ice formation, which, in turn, is driven by transport of ice from the shelf region to the open ocean. The water produced during sea ice formation mixes with warmer water from the open ocean pycnocline to form Shelf Water. *Gill* [1973] postulates that Shelf Water flows off the shelf by two processes: meridional overturning in geostrophic balance with an east-west pressure gradient, with on-shelf flow in the upper 200 m and off-shelf flow in the lower 300 m, and westward flow in a horizontal plane along the shelf edge. The sinking plume is close to being a contour current and takes about 1 year to reach the bottom. Bottom water is produced throughout the year, although brine production is seasonal. The flux at the edge of the shelf is about 2 Sv (1 Sv = 10^6 m^3 s^{-1}) but increases to 6-8 Sv through entrainment of surrounding water. Hydrographic sections presented by *Foster et al.* [1987] clearly show that Shelf Water sinks down the continental slope as a boundary layer plume of 100 to 200 m thickness. The coldest Shelf Water has a temperature of -1.8°C, while salinity varies from about 34.2‰ at the surface to up to 34.6‰ on the shelf bed. Entrainment of relatively warm and salty water from the open ocean as the plume flows down the continental slope results in bottom water with a temperature of -0.6°C to -0.8°C and a salinity of 34.62-34.64‰.

The properties of Shelf Water in the Weddell Sea and of the resultant AABW are influenced to some extent by interaction with the floating Ronne Ice Shelf. As discussed by *Jenkins and Doake* [1991] and *Jenkins* [1991], the Antarctic ice mass is grounded in the Weddell Sea at a depth of 1400 m. Shelf Water flows toward the grounding line, where it is warmer than the pressure melting point, causing melting at the ice base. This produces a plume of low salinity, supercooled and buoyant water called Ice Shelf Water (ISW), which flows outward underneath the upward sloping base of the ice shelf. Beginning about 300 km from the grounding line and at a depth of 600 m, basal freezing occurs, thereby increasing the ISW density. At a depth of about 400 m the ISW plume breaks free from the ice surface, at which point it has a temperature colder than -2°C. As this is colder than the surface freezing point, mixing of ISW with Shelf Water will cool the latter. The total flux of water leaving the Ronne Shelf is uncertain but could be about 0.8 Sv. In effect, the base of the ice shelf serves as a giant heat exchanger, cooling a portion of Shelf Water to temperatures lower than would otherwise be the case. *Jenkins and Doake* [1991] speculate that the greater shelf area available for conditioning of shelf waters in the Weddell Sea than in the Ross Sea might explain why the Weddell Sea is a more important source of AABW. Data presented by *Foldvik and Gammelsrod* [1988, Figure 9] indicate that the coldest plume temperature, -1.97°C, occurs at a depth of about 1400 m, suggesting that supercooled ISW water mixes directly with the sinking plume at this depth rather than first mixing with Shelf Water.

Although formation on continental shelves, as described above, appears to be the dominant mechanism of AABW formation, some AABW also appears to form by deep convection in the open ocean, as described by *Gordon* [1978] and *Killworth* [1979]. Broad regions are initially destabilized by upward doming of isopycnal surfaces by cyclonic eddies. Surface cooling to -1.9°C, followed by sea ice formation and brine ejection, creates water dense enough to mix to 2000 m depth in regions of 30-50 km diameter referred to as "chimneys"; the water produced by such overturning has T=-0.36°C and S=34.6‰. It is not clear, however, whether such mixing merely homogenizes the water column or is associated with a net downward mass flux which can feed a northward flowing AABW current.

Gill [1973] and *Foldvik and Gammelsrod* [1988], among others, have drawn attention to the importance of the greater compressibility of cold water relative to warm water in creating plumes dense enough to sink to the abyssal depths. Thus the density of relatively cold and fresh water

(which feeds the boundary layer plume) will increase faster with increasing depth than that of relatively warm and saline water (as found in the adjacent open ocean). Hence the density difference between the plume and the surroundings can initially increase with increasing depth, in spite of substantial entrainment of ambient water into the sinking plume.

North Atlantic Region

Bottom water in the North Atlantic is referred to as North Atlantic Deep Water (NADW), and the following three sources are recognized: water flowing over the sill (at approximately 600 m depth) in the Denmark Strait, between Greenland and Iceland, at T=1 °C and S=34.94‰; water flowing over the sill (at approximately 850 m depth) between Iceland and Scotland, at T=2-3 °C and S=35.0‰; and Labrador Sea Water (LSW), formed by deep convection in winter with T=3-4 °C and S=34.87‰ [*Swift*, 1984]. The source for Denmark Strait overflow water is thought to be surface water in the Greenland and Iceland Seas, although there is disagreement regarding the relative importance of these two source areas [*Swift et al.*, 1980; *Strass et al.*, 1993]. Iceland-Scotland overflow water originates from a mixture of relatively warm (6-8 °C) and saline (35.1-35.3‰) Atlantic water and cold (mostly < -0.4 °C) and fresh (34.0-34.94‰) Norwegian Sea Deep Water (NSDW) [*Swift*, 1984].

The Iceland-Scotland overflow water flows westward to the south of Iceland and joins Denmark Strait overflow off the coast of Greenland. On the basis of direct current measurements, *Dickson et al.* [1990] and *Dickson and Brown* [1994] estimate the overflow flux at 63 °N, where the two currents have joined, to be 10.7 Sv, with little seasonal or interannual variation. They endorse earlier estimates for the Denmark Strait and Iceland-Scotland overflow fluxes of 2.7 Sv and 2.5-2.9 Sv, respectively, which implies that the combined flux doubles by the time it reaches 63 °N as a result of entrainment. They believe that the flux increases further, to 13.3 Sv, by the time it passes the tip of Greenland (at 59 °N). Both Denmark Strait and Iceland-Scotland overflow water descend from their respective sill depths to a depth of about 2000 m, where they join, largely as contour currents, then descend farther to in excess of 3000 m depth off Newfoundland. *McCartney and Talley* [1984] developed a three-box model of the North Atlantic region in order to estimate volume fluxes based on water mass properties and estimated air-sea heat exchange. They conclude that the combined Denmark Strait and Iceland-Scotland overflow is only 1.7 Sv, with entrainment adding another 0.8 Sv. However, they believe that the combined flux of 2.5 Sv is augmented by a further 8.6 Sv of Labrador Sea Water, giving a total flux at 50 °N of 11.1 Sv. Other estimates cited by *McCartney and Talley* [1984] and based on a variety of techniques indicate a total southward flux of cold (<4 °C) deep water in the Atlantic Ocean of 12-18 Sv between latitudes 24 °N and 53 °N, while alternative assumptions (within the bounds of observational uncertainty) yield a total flux as large as 14.1 Sv using *McCartney and Talley*'s [1984] method.

Model Description

In this section the plume model adopted here is described in detail. The energy balance surface climate model and sea ice and ocean models, to which the plume model is coupled, are briefly described. Details concerning the ocean model are given by *Harvey* [1992], while details concerning the surface climate and sea ice models are given by *Harvey* [1988a, b].

Surface Climate, Sea Ice, and Ocean Models

The energy balance climate model has surface-air, land-sea, and latitudinal resolution and is forced with diurnally averaged but seasonally varying insolation. The surface layer in the oceanic part of each zone consists of an isothermal mixed layer which here is assumed to be 75 m thick except in the polar shelf regions, as explained below. Meridional transport of heat in the atmosphere occurs by diffusion. The latitudinal and seasonal variation of precipitation is prescribed from observations and scaled so that global precipitation equals global evaporation on each time step. Zonally averaged zonal surface winds are also prescribed from observations and used as an upper boundary condition to the ocean model. Surface-air fluxes of latent and sensible heat are computed from bulk aerodynamic formulae with a stability-dependent drag coefficient. Vertical growth of sea ice is computed using *Semtner*'s [1976] zero-layer model with minor modifications.

The ocean model consists of a zonally averaged deep ocean between latitudes ϕ_N=66 °N and ϕ_S=74 °S, with a depth here of 3800 m between 58 °N and 66 °N, 4800 m between 30 °N and 74 °S, and a linear variation between 30 °N and 58 °N. As explained in *Harvey* [1992], the ocean model solves the zonally averaged, steady state form of the equations of motion through the introduction of a stream function and the parameterization of the component of the zonal pressure gradient due to density variations in terms of the component of the meridional pressure gradient due to density variations, as in the work by *Wright and Stocker* [1991].

The treatment of the Drake Passage, between South America and Antarctica at 54 °S-62 °S, is critical to the global scale thermohaline circulation and hence to the vertical gradients of temperature and salinity next to the polar limits of the deep ocean, where plumes can form. *Harvey* [1992] neglected the subsubsurface sill in the Drake Passage, but it must be included here to permit adequate interaction between plume water poleward of the Drake Passage and deep water on the equatorward side of the passage. We therefore allow for the existence of a subsurface sill in the Drake Passage at a depth of 2475 m. Above the sill the zonal mean zonal pressure and hence density gradient must be zero, but it is nonzero below the sill, with a discontinuity at the sill depth z_s. Following *Wright and Stocker* [1992], the zonal density gradient P is given by

$$\frac{\partial P}{\partial \lambda} = \begin{cases} \dfrac{\partial P}{\partial \lambda}\Big|_{z_1} - g\int_{z_1}^{z}\left(\dfrac{\partial \rho}{\partial \lambda}\right)_i dz' & z_1 \le z \le z_s \\ 0 & z > z_s \end{cases} \tag{1}$$

where

$$\left(\frac{\partial \rho}{\partial \lambda}\right)_i = -2\sin\phi\cos\phi\epsilon\frac{\partial \rho}{\partial \phi} \tag{2}$$

with ε=0.15 in the Drake Passage. Substituting (1) and (2) into *Harvey* [1992, equation (1)], integrating piecewise over the entire column, and applying the boundary conditions that $\rho A u_z = \tau$ at the upper boundary ($z=z_2$) and $A u_z = cu$ at the lower boundary ($z=z_1$) (where τ is the fixed zonal surface wind stress, ρ is density, A is the vertical viscosity coefficient, u is the zonal velocity, and c is a friction coefficient), one can form an equation for $\partial P/\partial\lambda|_{z_1}$. Substituting this equation back into (1) yields

$$\frac{\partial P}{\partial \lambda} = \begin{cases} 2\sin\phi\cos\phi \int_{z_1}^{z} e\left(\frac{\partial \rho}{\partial \phi}\right) dz' \\ \quad - \frac{2\sin\phi\cos\phi g}{H_R} \int_{z_1}^{z_s}\int_{z_1}^{z} e\left(\frac{\partial \rho}{\partial \phi}\right) dz' dz \\ \quad + \frac{\rho r \cos\phi}{H_R}\left(\frac{\tau}{\rho} - cu_1\right) & z_1 \le z \le z_s \\ 0 & z > z_s \end{cases} \quad (3)$$

where $H_R = z_s - z_1$. As derived by *Harvey* [1992], the stream function ψ is given by

$$\psi(z) = \frac{Ag}{\rho f^2 r}\frac{\partial \rho}{\partial \phi} - \int_{z_1}^{z} \frac{1}{\rho f r \cos\phi}\frac{\partial P}{\partial \lambda} dz' - \frac{cu_1}{f} \quad (4)$$

where f is the Coriolis parameter and r is the Earth's radius. Substituting (3) into (4) and setting $cu_1 = \tau/\rho$ so as to give continuity of ψ at $z=z_s$ yields

$$\psi = \begin{cases} \frac{gA}{\rho f^2 r}\frac{\partial \rho}{\partial \phi} - \frac{\tau}{\rho f} + \frac{2\sin\phi g}{\rho f r}\left[\left(\frac{z-z_1}{H_R}\right)\int_{z_1}^{z_s}\int_{z_1}^{z} e\left(\frac{\partial \rho}{\partial \phi}\right) dz' dz \right. \\ \quad \left. - \int_{z_1}^{z}\int_{z_1}^{z'} e\left(\frac{\partial \rho}{\partial \phi}\right) dz'' dz'\right] & z_1 \le z \le z_s \\ \frac{gA}{\rho f^2 r}\frac{\partial \rho}{\partial \phi} - \frac{\tau}{\rho f} & z > z_s \end{cases} \quad (5)$$

By comparison, at latitudes where a continent is present, ψ is given by

$$\psi = \frac{gA}{\rho f^2 r}\frac{\partial \rho}{\partial \phi} - \left(\frac{z-z_1}{D}\right)\frac{\tau}{\rho f} - \frac{2\sin\phi g}{\rho f r}\left[\left(\frac{z-z_1}{D}\right)\int_{z_1}^{z_2}\int_{z}^{z_2} e\left(\frac{\partial \rho}{\partial \phi}\right) dz' dz - \int_{z_1}^{z}\int_{z'}^{z_2} e\left(\frac{\partial \rho}{\partial \phi}\right) dz'' dz'\right] \quad (6)$$

where $D = z_2 - z_1$.

Whenever an unstable potential density profile occurs between any two layers, convective overturning is assumed to occur and to establish uniform temperature and salinity over the unstable depth interval. On the basis of *Gargett* [1984], the vertical diffusion coefficient K_v is parameterized in terms of the local Brunt-Väisälä frequency N as

$$K_v = \frac{A_0}{N} \quad (7)$$

Here, we will present results using $A_0 = 0.5 \times 10^{-7}$ m^2 s^{-2} and $A_0 = 2 \times 10^{-7}$ m^2 s^{-2}. The former results in K_v varying from about 0.1 cm^2 s^{-1} at the surface to 1-2 cm^2 s^{-1} near the ocean bottom outside regions of convection, while the latter results in K_v with values in excess of 1 cm^2 s^{-1} below about 600 m depth and reaching 10 cm^2 s^{-1} at the ocean bottom. In both cases, K_v approaches the imposed upper limit of 100 cm^2 s^{-1} in regions of convection. The horizontal diffusion coefficient K_h is set to O(10^4) m^2 s^{-1} within the mixed layer but is parameterized in terms of N below the mixed layer, as in *Harvey* [1995], and ranges from about 1 x 10^3 m^2 s^{-1} throughout most of the ocean to an imposed lower limit of 1 m^2 s^{-1} in regions of convection. The diffusion coefficients for heat and salt are assumed to be equal, and the vertical viscosity coefficient A is assumed to be equal to K_v (with the constraint $A \le 10^{-2}$ m^2 s^{-1}).

The mixed layer serves as an upper boundary to the deep ocean domain; governing equations for temperature and salinity are given by *Harvey* [1992]. The effect of evaporation, precipitation, and runoff is represented by an equivalent salt flux rather than by a water mass flux. The Antarctic ice mass is assumed to be in mass balance, so annual net snowfall on Antarctica is assumed to be balanced by ice shelf calving; the water mass associated with calving is added to runoff between latitudes 74°S and 82°S.

Polar Plume Model

We assume that a northern hemisphere (NH) polar plume originates from a shelf at 700 m depth between latitude 66°N and 74°N, while a southern hemisphere (SH) plume originates from a shelf at 450 m depth between latitudes 74°S and 82°S. The plumes subsequently slide down the continental slope. The initial plume flux at the break between the polar shelf and continental slope, $F(z_{shelf})$, is computed once per year as

$$F(z_{shelf}) = \gamma(Q_e + Q_i^* + Q_c) \quad (8)$$

where γ is a tunable parameter, Q_e is the volumetric annual net evaporation over the shelf, summed only when gross evaporation minus precipitation and runoff is positive; $Q_i^* = (30/35)Q_i$, where Q_i is the volumetric annual net freezing over the shelf area, summed only when positive, and Q_c is given by

$$Q_c = \frac{\partial \rho/\partial T}{\rho L_c \partial \rho/\partial S}\int_{shelf}\int_{year} MAX(0, R^*) dt dA \quad (9)$$

where R^* is the net surface-to-air heat flux (including radiative fluxes). Q_c is expressed as the volume of evaporation having the same effect on mixed layer density as the cooling that occurs. In the zonally averaged model used here some sea ice formation occurs in the latitude zone corresponding to the NH shelf, but we set Q_i=0.0 in the NH because sea ice formation does not occur at the longitudes where the NH plume forms in the real world (this is acceptable because only warming perturbations are considered here). The terms Q_e, Q_i, and Q_c represent the processes which can lead to dense waters on the bottom of the shelf, while γ accounts for the flow of water from the open ocean pycnocline onto the shelf and its mixing with shelf water. The ice freezing, evaporation, and cooling forcings are summed only over time steps when net ice formation, evaporation, or mixed layer cooling occurs because at these times, surface water is made denser and can sink, while at other times, surface water is made lighter and will not sink. The flow from the open ocean to the

shelf is assumed to occur uniformly between the surface and the shelf depth and to decrease linearly with distance from the equatorward to poleward edge of the shelf. Since changes in ice mass or evaporation do not lead to changes in ocean mass in the model presented here, consistency requires that the plume flux off the shelf equal the net flow onto the shelf from the open ocean pycnocline.

The initial plume temperature is given by the mean temperature of the shelf waters which contribute to the plume, while the initial plume salinity is assumed to be equal to the mean salinity of water flowing onto the shelf plus an offset ΔS. *Toggweiler and Samuels* [1995] indicate that the difference in salinity between waters flowing onto and off the Weddell and Ross Sea shelves is 0.15-0.2‰, so we use ΔS=0.2‰ in the SH. Hydrographic sections across the flow path of the North Atlantic plumes, on the other hand, indicate no significant salinity enhancement compared to the adjacent water masses [i.e., *Clarke and Gascard*, 1983, Fig.4; *Dickson and Brown*, 1994, Figure. 3], so we use ΔS=0.0‰ in the NH.

To account for conditioning of SH plume source waters by interaction with the Ronne Ice Shelf, the temperature of 25% of the plume flux at the shelf brink is reduced to -1.9°C and assumed to mix with the remaining plume water (that is, the mean plume temperature is reduced by 25% of the difference between the initial temperature and -1.9°C). In order to conserve energy, an equivalent amount of heat is added to the atmosphere over Antarctica. Interaction with the Ronne Ice Shelf is assumed to have no net effect on plume salinity, since melting of the ice shelf base during the first part of the plume source water flow path would be largely balanced by basal freezing prior to separation of the plume flow path from the base of the shelf and because we already assume that net snow accumulation on Antarctica is exactly balanced by ice calving and melting in the shelf region.

The equations governing the along-slope plume velocity u and cross-slope velocity v once the plume crosses the shelf brink are:

$$-C_D(u^2+v^2)^{1/2}v - h\frac{g\alpha\Delta\rho}{\rho_o} - \frac{h}{\rho_o}\frac{\partial P}{\partial y} - fuh = 0 \quad (10)$$

$$-C_D(u^2+v^2)^{1/2}u - \frac{h}{\rho_o}\frac{\partial P}{\partial x} + fvh = 0 \quad (11)$$

where α is the continental slope ($\alpha > 0$ in the NH and < 0 in the SH), $\Delta\rho$ is the density difference between the plume and surrounding water, ρ_o = 1027 kg m^{-3} is a typical plume density, C_D is a bottom drag coefficient, and h is the plume thickness. As suggested by *Gill* [1973], $\Delta\rho$ is computed based on actual rather than potential densities. Equation (10) represents a balance between drag on the plume, the downslope negative buoyancy, the external pressure gradient, and the Coriolis force, while (11) includes all the above terms except the buoyancy term. The meridional pressure gradient is determined from the ocean model, but the zonal pressure gradient acting on the plume must be externally prescribed here. It represents both dynamical effects due to barriers to the zonal plume velocity component and zonal variation in the salinity of shelf water due to regional variation in evaporation and sea ice forcing.

Changes in plume mass flux M_f per unit width are given by

$$\frac{d}{ds}(M_f) = E_o(u^2+v^2)^{1/2} \quad (12)$$

where s is distance along the plume flow path and E_0 is a dimensionless entrainment parameter. The closure assumption adopted above to compute changes in plume mass flux is the same as that adopted by *Smith* [1975] and *Killworth* [1977]. Alternative closure assumptions, such as determining plume thickness by requiring that the plume Richardson number be less than or equal to unity, as in the work by *Trowbridge and Lentz* [1991], could also be invoked. If Δz is the thickness of a given model layer, then $\Delta s' = \Delta z/|\alpha|$ is the distance directly down the continental slope as the plume sinks through the model layer and $\Delta s = \Delta s'\sqrt{(1+(u/v)^2)}$ is the distance along the flow path as the plume sinks through the model layer. The plume thickness h is given by

$$h = \frac{M_f}{(u^2+v^2)^{1/2}} \quad (13)$$

Finally, the plume flux at depth z, $F(z)$, is given by

$$F(z) = wM_f \quad (14)$$

where w is the plume width. From (12) and (14) it follows that, for given u and v, the downslope change in the plume mass flux will be constant when w is altered if wE_0 is constant. Given that the initial plume flux is independently determined using (8), a larger w implies a smaller h. However, there will be no net effect on the u and v solutions if C_D/h and hence wC_D are constant as w varies. The values of C_D and E_0 required to produce a given plume flux variation depend on the choice of w, but a given solution is preserved as the assumed w varies if appropriate changes in C_D and E_0 are made: the values given later assume that w spans 1/4 of the shelf edge length.

To solve the above system of equations, we cast (10) and (11) in prognostic finite difference form and eliminate h through use of (13). Given the values of M_f, u, and v at the base of the previous model layer, we repeatedly apply the prognostic equations with 1000-s time steps until u and v have converged to constant values. This normally takes about 20-40 steps, during which time the plume would have traversed only a small fraction of the model layer. We then compute the change in mass flux ΔM_f as the plume traverses the current model layer, where

$$\Delta M_f = E_o\left(\frac{u^2+v^2}{v}\right)\Delta s' \quad (15)$$

This process is repeated as the plume descends through successive model layers until either $\Delta\rho < 0$, $|v| < 10^{-4}$ m s^{-1}, or the lowest model layer is reached, at which point detrainment of the plume is assumed to occur.

The plume submodel affects the two-dimensional flow field predicted by the ocean model directly through mass fluxes out of or into the sides of the ocean model domain and indirectly through the effect on the temperature and salinity fields of the injection of plume water at depth.

Results

We first compare the model flow field and temperature profile for cases with and without plumes, then we compare the transient and steady state surface temperature and sea

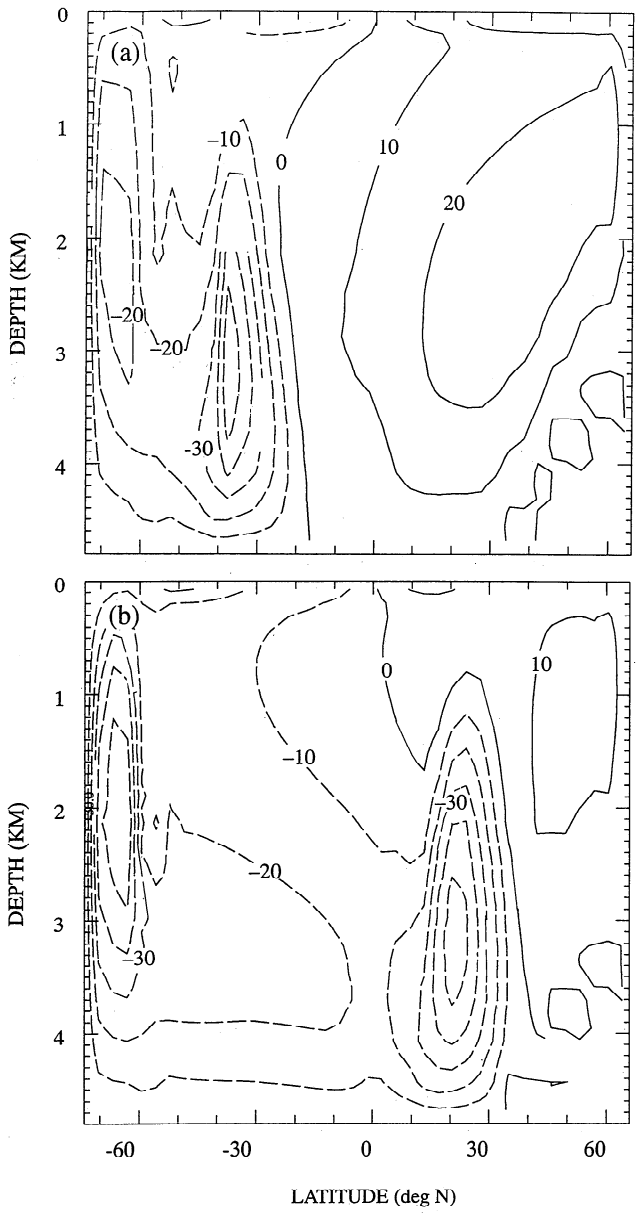

Figure 1. Latitude-depth flow field (in sverdrups, where 1 Sv=10^6 m^3 s^{-1}) for the following cases: (a) spin-up without polar plumes and (b) steady state response to a 4 W m^{-2} heating perturbation without plumes.

level response to a greenhouse gas (GHG) increase for cases with and without polar plumes.

Steady State Spin-up

In the absence of the Drake Passage the thermohaline circulation obtained by the two-dimensional model without plumes usually consists of a single overturning cell spanning both hemispheres, with concentrated downwelling next to one polar boundary and upwelling throughout the opposing hemisphere. The upwelling, in turn, establishes a strong vertical salinity gradient (with salinity decreasing upward) next to the polar edge of the deep ocean. This, in turn, makes it impossible for a plume to be dense enough to sink to the ocean bottom using a realistic ΔS. The hemisphere in which upwelling occurs and hence in which deep plumes are precluded depends on the choice of heat diffusion coefficient in the mixed layer and on the vertical diffusion coefficient, with an abrupt flip-flop in the direction of thermohaline overturning as either of these parameters is varied. The occurrence of a single overturning cell has been noted even in hemispherically symmetric ocean models [*Bryan,* 1986]. The inability to form plumes in both hemispheres in this case indicates that simulation of realistic plumes in global ocean GCMs will be critically dependent on the large-scale salinity and temperature fields simulated by the model and that use of an overly idealized model (such as idealized geography or bathymetry) can prevent realistic plumes from forming.

Inclusion of the Drake Passage but with no subsurface sill allows the establishment of an isolated, intense overturning cell poleward of the Drake Passage, with downwelling next to the polar limit of the deep ocean. This, in turn, allows deep plumes to form in both hemispheres. However, significant mass exchange between this polar cell and the main overturning cell requires a subsurface sill, which allows a zonal pressure gradient below the sill depth and the establishment of geostrophic meridional currents. Figure 1a shows the flow field for the case with a Drake Passage having a subsurface sill at a depth of 2475 m but without plumes for A_0=0.5 x 10^{-7} m^{-2} s^{-2}. When plumes are permitted, the intensity of both overturning cells decreases by a modest 20%, which implies that the lateral spreading of plume water along the ocean bottom and its upwelling have reduced the meridional gradient of density by the same fraction. Apart from the reduction in overturning intensity, the introduction of plumes has simply resulted in about half of the concentrated downwelling mass flux next to the polar boundaries becoming part of the plume mass flux, with little qualitative change in the flow field.

The adjustable parameters in the plume model are γ, which determines the relationship between the initial plume mass flux and plume forcings; E_o, which influences the rate of change of plume mass flux and density due to entrainment; the drag coefficient C_D; and the cross-slope pressure gradient $\partial P/\partial x$. Table 1 lists the parameter values for each hemisphere used here, while Table 2 lists the forcings and properties of the plumes produced here. In the NH the ice forcing is zero by design and the cooling forcing is largest, while in the SH, net sea ice freezing is overwhelmingly dominant, with surfacing cooling and evaporation playing minor roles. Both plumes have reasonable entrainment, with the NH plume being warmer and saltier than the SH plume (although the salinity difference and absolute salinities are somewhat too large). These

Table 1. Base Case Parameter Values Adopted

Parameter	NH Value	SH Value
γ	32	32
E_o	0.004	0.002
C_D	0.008	0.008
$\partial P/\partial x$	-1.0 x 10^{-6}	-1.0 x 10^{-6}

All parameters are dimensionless except for $\partial P/\partial x$, which has units of kg m^{-2} s^{-2}. NH is northern hemisphere, and SH is southern hemisphere.

Table 2. Basc Casc Plume Forcings and Various Properties

Property	NH Plume	SH Plume
Q_e, Sv	0.038	0.003
Q_i, Sv	0.000	0.086
Q_c, Sv	0.060	0.008
Initial flux, Sv	3.13	3.92
Initial T, °C	-0.43	-1.95
Initial S, ‰	35.42	35.05
Final flux, Sv	11.19	7.86
Final T, °C	1.20	-1.91
Final S, ‰	35.41	34.96

Q_e is evaporative forcing, Q_i is sea ice forcing, and Q_c is surface cooling forcing. Flux refers to plume flux.

results demonstrate that it is possible, in a simple, zonally averaged ocean-atmosphere model framework, to simulate polar plumes that sink to the ocean bottom with a realistic entrainment en route and with appropriate differences between the two hemispheres.

Table 3 compares the salinity budget for the shelf regions in the two hemispheres. Net melting of ice occurs over the NH shelf during the course of a year, thereby tending to reduce the shelf salinity, whereas net freezing occurs over the SH shelf. The primary balance in the SH is between salinification due to net ice freezing and freshening due to ice calving, in agreement with observational analysis of *Toggweiler and Samuels* [1995], while the primary balance in the NH is between freshening due to ice melting and salinification due to mixing with Atlantic water.

Sensitivity to Parameter Changes

The depth of plume detrainment and the flux at detrainment are remarkably insensitive to a halving or doubling of each of the tunable parameters listed in Table 1. A fourfold variation in γ causes a corresponding variation in the initial plume flux but only a factor of 2 (SH) or 3 (NH) variation in the flux at detrainment. This reduction in flux sensitivity occurs because, as γ and the initial flux increase, so does the initial plume thickness, so that subsequent entrainment is less important in relative terms. Similarly, as E_0 increases by a factor of 4, the flux at detrainment increases by only 30-100%; in this case, a larger E_0 is offset by reduced plume bouyancy and flow speed, which is a counteracting effect on entrainment. Finally, a factor of 4 variation in C_D, and $\partial P/\partial x$ produces only a 10-20% variation in the detrainment flux. In almost all cases the plumes are able to penetrate to the ocean bottom in each hemisphere.

Table 3. Salinity Budget for the Shelf Regions

Process	NH	SH
Plume formation	0.0000	0.0089
Meridional diffusion	-0.0129	0.0053
Runoff plus calving	0.0072	0.0320
Net precipitation	-0.0024	-0.0033
Freezing	0.0103	-0.0430

Values are expressed as the annual depth (in meters) of fresh water added.

Flow, Temperature and Sea Level Response to a GHG Increase

We mimic the effect of a sudden GHG increase by imposing a step-function, latitudinally and seasonally uniform reduction ΔQ to the infrared emission to space, and by increasing the downward infrared emission from the atmosphere to the surface by $\Delta Q/6$, as the work by *Harvey* [1994]. As climate warms, the initial plume flux will change due to changes in the sea ice, evaporative, and surface cooling forcings, but the parameter γ is held constant. Changes in the plume at greater depth will occur due to differences in the initial plume density and in the ambient water as the model climate warms. We assume that interaction with the Ronne Ice Shelf continues to cool 25% of the SH plume flux at the shelf brink to -1.9°C, although for large heating perturbations this could eventually change due to changes in the Antarctic ice mass.

The dominant factor in the global mean deep ocean warming, in sea level rise, and in the latitudinal variation of the surface temperature response to the heating perturbation is the fact that for all heating perturbations considered and for cases with and without plumes, there is a progressively greater weakening of the NH thermohaline driven overturning cell and an expansion in the size of the SH cell as the heating perturbation increases. For ΔQ=4 W m^{-2} and larger the NH cell almost completely disappears, as illustrated in Figure 1b. This response is found to be a robust feature of the model simulation, in that it occurs for widely differing values of K_h, K_v, and ε. On the other hand, use of less realistic land-sea geography or in the treatment of the Drake Passage and the SH shelf region can eliminate this behavior. The collapse of the NH cell is driven, in the present model, by the greater downward penetration of the surface warming anomaly at high latitudes due to the fact that the circulation is downwelling at high latitudes. This, in turn, reduces the meridional density gradient at depth, which thereby reduces the overturning circulation intensity. Note that this circulation weakening is not dependent on increased precipitation at high latitudes, as the precipitation pattern is fixed in the present model; as illustrated by *Manabe and Stouffer* [1995], changes in freshwater inputs are another potential cause of a reduced thermohaline overturning intensity.

When plumes are permitted, a similar collapse of the NH thermohaline overturning cells occurs. The total plume forcing decreases by about 30% in both hemispheres as ΔQ increases to 8 W m^{-2}, the NH hemisphere plume detrains at a depth of about 1000-1200 m for ΔQ=4 W m^{-2} and larger, and the SH plume continues to sink to the ocean bottom before detraining. The continued formation of a plume with partial sinking in the NH, while the thermohaline overturning in the open ocean largely collapses, explains a number of modest differences between the cases with and without plumes, which are discussed below.

Since both cells transport heat to their respective polar regions, the weakening of the NH cell and strengthening of the SH cell suppress the steady state warming at high latitudes in the NH but strengthen it in the SH, as illustrated in Figure 2 for ΔQ=4 W m^{-2} and ΔQ=6 W m^{-2}. The presence of plumes has a significant effect on the high-latitude temperature response in the NH. In the case without plumes the steady state warming around 60°N decreases as ΔQ

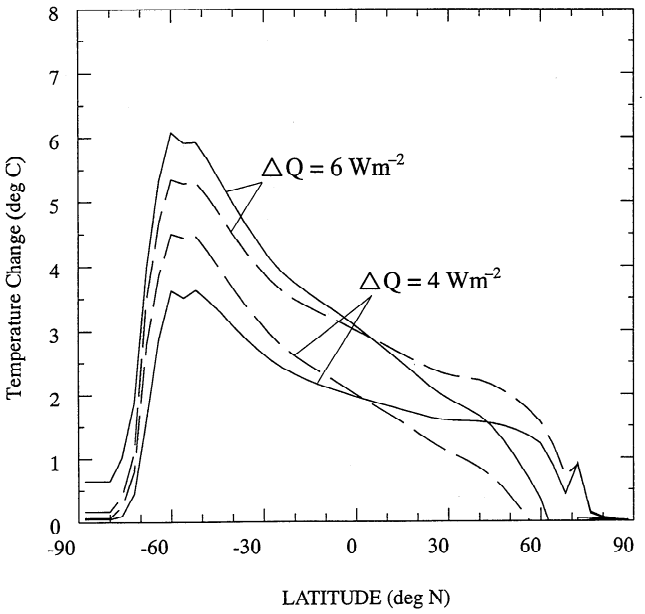

Figure 2. Latitudinal variation of mean annual mixed layer temperature response to heating perturbations ΔQ of 4 W m^{-2} and 6 W m^{-2} with A_0=0.5 x 10^{-7} m^2 s^{-2} for cases without plumes (solid lines) and with plumes (dashed lines).

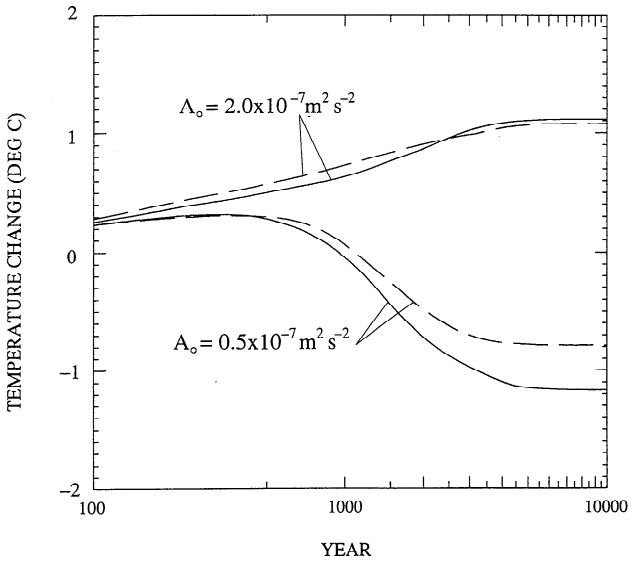

Figure 3. Transient global mean deep ocean warming for ΔQ=6 W m^{-2} and A_0=0.5 x 10^{-7} m^2 s^{-2} or A_0=2.0 x 10^{-7} m^2 s^{-2} for cases without plumes (solid lines) and with plumes (dashed lines).

increases from 4 to 6 W m^{-2}, as the local effect of weakened overturning overrides the effect of increased greenhouse heating. In the case with plumes the poleward heat flux is more resilient, so that high latitude warming increases as the heating perturbation increases from 4 W m^{-2} to 6 W m^{-2}. These quantitative results should not be taken literally; rather, they indicate that the incorporation of plumes in three-dimensional models could have important regional effects including, in particular, the extent and impact of a shutdown of the overturning circulation in the North Atlantic Ocean.

Since sinking water from the NH cell and plume is warmer than sinking water from the SH cell and plume, the change in relative cell strength tends to cause a cooling of the deep ocean as the surface climate warms, with a corresponding fall in sea level due to thermal effects on the density of seawater. The deep ocean cooling tendency is offset by additional downward heat diffusion as the surface warms, an effect which is stronger when A_0 and hence K_v is larger. These features are illustrated in Figure 3, which shows the global mean deep ocean warming and sea level rise for ΔQ= 6 W m^{-2} using A_0=0.5 x 10^{-7} m^{-2} s^{-2} and A_0=2 x 10^{-7} m^{-2} s^{-2}, and in Figure 4, which shows the vertical profile of global mean ocean warming. With the small A_0 a mean ocean cooling occurs for ΔQ of 2-6 W m^{-2}, with the cooling and heating tendencies cancelling out in the mean when ΔQ=8 W m^{-2} to give no change in mean deep ocean temperature, while for the large A_0 this cancellation occurs around ΔQ=4 W m^{-2}. Thus Figure 3 shows a mean deep ocean cooling for small A_0 of about 1 °C and a mean deep ocean warming of about 1 °C for large A_0. The presence of plumes has a modest effect on the mean deep ocean warming with small A_0 but very little effect with large A_0, where diffusion is stronger.

Figure 5 shows the latitude-depth variation in steady state deep ocean temperature change for ΔQ=4 W m^{-2} and A_0=0.5 x 10^{-7} m^2 s^{-2}. The expansion of the relatively cold SH cell into the NH causes deep ocean cooling to occur in a broad band at low latitudes; this cooling belt extends from the ocean bottom to within a few hundred meters of the surface and is flanked by warming on both sides. Steady state cooling at low latitudes in the NH and warming at high latitudes maintain the reduction in meridional density gradient that arose during the early stage of the transient response due to the initially faster downward penetration of the heating anomaly at high latitudes. For this reason, the collapse of the NH circulation cell becomes self perpetuating. In contrast, in the greenhouse gas heating pertubation

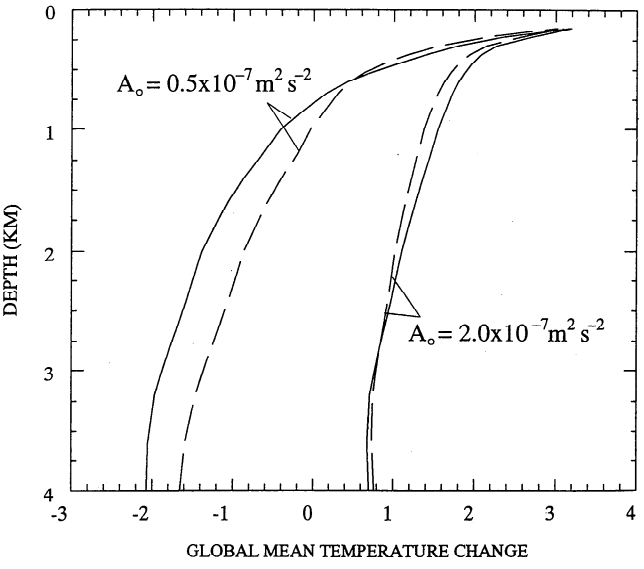

Figure 4. Comparison of globally averaged steady state deep ocean temperature profiles for ΔQ of 6 W m^{-2} and A_0=0.5 x 10^{-7} m^2 s^{-2} or A_0=2.0 x 10^{-7} m^2 s^{-2} for cases without plumes (solid lines) and with plumes (dashed lines).

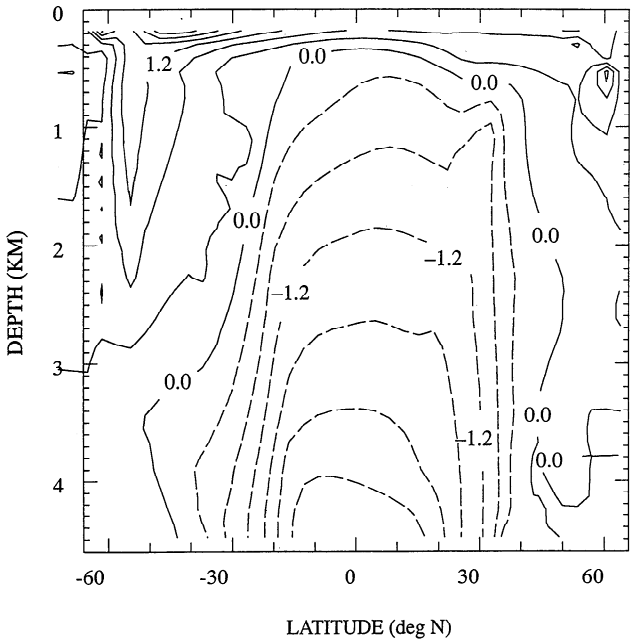

Figure 5. Steady state temperature change field for ΔQ of 4 W m^{-2} and A_0=0.5 x 10^{-7} m^2 s^{-2} for the case without plumes.

experiments presented by *Harvey* [1994], the transient circulation collapse was always accompanied by a reinvigoration of the circulation in steady state (albeit after a lag of up to 1000 years). Thus whether a transient circulation collapse becomes permanent or not depends on the nature of the circulation that becomes established during the transient, which, in turn, depends on the model geometry and initial flow field and climate.

Figure 6 compares the variation in maximum stream function value for the ΔQ=4 W m^{-2} and A_0=2.0 x 10^{-7} m^2 s^{-2} case. The maximum stream function value is an indicator of the overall overturning intensity, and the results shown in Figure 6 illustrate the general result that the flow variability is greater when plumes are permitted to form. This, in turn, can be related to the shorter timescales involved in changes in the plume forcing factors compared to the large-scale meridional density gradient, which drives the overturning circulation outside the plumes.

The original motivation in formulating a plume submodule was the expectation that the model version with plumes would show a smaller deep ocean warming and, consequently, a smaller sea level rise due to thermal expansion. This expectation in turn was based on the expectation that the plume source waters would show smaller warming, at least for small enough ΔQ, than the water poleward of the shelf regions and substantially smaller warming than the global mean mixed layer. This latter expectation is indeed the case; as ΔQ increases from 2 to 8 W m^{-2}, the mean mixed layer warming increases from 1.1 to 4.4°C, the NH plume source temperature warms by only 0.2-1.4°C, and the SH plume source temperature warms by 0.0°C for ΔQ=2-4 W m^{-2} and by 1.4°C for ΔQ=8 W m^{-2}. Warming is also suppressed, to a smaller extent, in the sinking regions adjacent to the shelves (58-66°N and 66-74°S), as can be seen from Figure 2. These difference would indeed have been sufficient to reduce deep ocean warming for the case with plumes except for the fact that the relative strength of the NH and SH source fluxes changes dramatically as the climate warms, and this overwhelms the impact of the limited warming of the plumes. Had the NH plume been able to persist as the overturning circulation in the open ocean collapsed, we might have seen a greater difference between plume and no-plume cases, but, as discussed in the context of the spin-up results, a downwelling circulation next to the plume region is needed in order to establish the minimal vertical density gradient needed to allow deep sinking of the plume. Thus the near-total collapse of this downwelling in the NH also shuts off deep plume sinking. In other words, the overturning circulation in the open ocean and the formation of deep plumes are intimately interconnected.

Conclusions

In this paper the role of boundary layer plumes that are driven by net ice formation, evaporation, and surface cooling on polar shelves and that are able to sink down the continental slope to the ocean bottom has been investigated using a two-dimensional (latitude-depth) ocean model coupled to simple energy balance surface climate and sea ice models. A long series of observational studies indicates that the formation of boundary layer plumes on polar continental slopes is a key process in ocean bottom water formation. However, no global ocean GCM to date includes this process. Rather, ocean GCMs produce bottom water only as a result of the large-scale thermohaline overturning, which is driven by horizontal density contrasts, or as a result of convective overturning, which is driven by vertical density contrasts.

The purpose here is not to obtain definitive answers concerning the role of polar plumes in climate and climatic change but, rather, to suggest their possible impacts and to

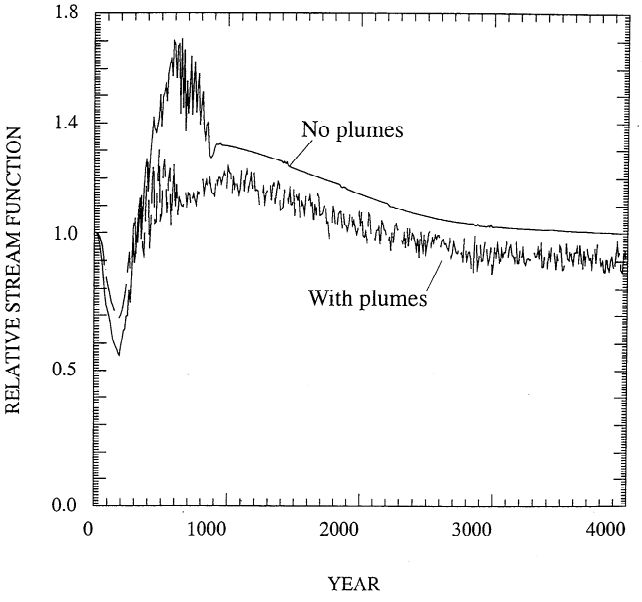

Figure 6. Relative variation in maximum stream function following a step function greenhouse gas heating perturbation ΔQ of 6 W m^{-2} and A_0=0.5 x 10^{-7} m^2 s^{-2} for the case without plumes (dashed lines) and with plumes (solid lines).

motivate routine inclusion of polar plumes in three-dimensional ocean GCMs.

An important lesson that emerges from the present study is that the correct simulation of the large-scale density field is essential to the simulation of realistic plumes in both hemispheres. In the two-dimensional model used here the impact of a shutdown in the NH thermohaline overturning cell dominated the transient and steady state climate and sea level response to greenhouse gas heating perturbations. In particular, mean deep ocean temperature tended to decrease due to the increase in the importance of cold Antarctic bottom water relative to warm NH bottom water. The inclusion of plumes in the present model did not significantly alter this basic response; however, the inclusion of plumes did have an important effect on the surface temperature response near 60°N. Given the potential importance of a shutdown in the North Atlantic overturning circulation to the regional climatic response to greenhouse gas increases and the possibility that regional climatic changes could be significantly modified through the inclusion of plumes in a model with longitudinal resolution, the incorporation of plume physics in global scale coupled atmosphere-ocean GCMs would seem to be a worthwhile task. However, on the basis of the results presented here, the inclusion of plumes in coupled three dimensional models is less important than the correct simulation of the overall ocean density field and the surface forcing conditions.

Acknowledgments. This research was supported by NSERC grant OPG0001413 and benefited from useful comments by J.R. Toggweiler and an anonymous reviewer.

References

Bryan, F., High-latitude salinity effects and interhemispheric thermohaline circulation. *Nature, 323,* 301-304, 1986.

Carmack, E.C., and T.D. Foster, On the flow of water out of the Weddell Sea, *Deep Sea Res., 22,* 711-724, 1975.

Clarke, R.A., and J.-C. Gascard, The formation of Labrador Sea Water, I, Large-scale processes, *J. Phys. Oceanogr., 13,* 1764-1778, 1983.

Dickson, R.R., and J. Brown, The production of North Atlantic Deep Water: Sources, rates, and pathways, *J. Geophys. Res., 99,* 12,319-12.341, 1994.

Dickson, R.R., E.M. Gmitrowicz, and A.J. Watson, Deep-water renewal in the northern North Atlantic, *Nature, 344,* 848-850, 1990.

Foldvik, A. and T. Gammelsrod, Notes on Southern Ocean hydrography, sea-ice and bottom water formation, *Palaeogeogr. Palaeoclimatol. Palaeoecol., 67,* 3-17, 1988.

Foster, T.D., and J.H. Middleton, Bottom water formation in the western Weddell Sea, *Deep Sea Res., 27A,* 367-381, 1980.

Foster, T.D., A. Foldvik, and J.H. Middleton, Mixing and bottom water formation in the shelf break region of the southern Weddell Sea, *Deep Sea Res., Part A, 34,* 1771-1794, 1987.

Gargett, A.E., Vertical eddy diffusivity in the ocean interior, *J. Mar. Res., 42,* 359-393, 1984.

Gill, A.E., Circulation and bottom water production in the Weddell Sea, *Deep Sea Res., 20,* 111-140, 1973.

Gordon, A.L., Deep Antarctic convection west of Maud Rise, *J. Phys. Oceanogr., 8,* 600-612, 1978.

Gordon, A.L., B.A. Huber, H.H. Hellmer, and A. Ffield, Deep and bottom water of the Weddell Sea's western rim, *Science, 262,* 95-97, 1993.

Harvey, L.D.D., A semianalytic energy balance climate model with explicit sea ice and snow physics, *J. Clim., 1,* 1065-1085, 1988a.

Harvey, L.D.D., Development of a sea ice model for use in zonally averaged energy balance climate models, *J. Clim., 1,* 1221-1238, 1988b.

Harvey, L.D.D., A two-dimensional ocean model for long-term climatic simulations: Stability and coupling to atmospheric and sea ice models, *J. Geophys. Res., 97,* 9435-9453, 1992.

Harvey, L.D.D., Transient temperature and sea level response of a two-dimensional ocean-climate model to greenhouse gas increases, *J. Geophys. Res., 99,* 18,447-18,466, 1994.

Harvey, L.D.D., Impact of isopycnal diffusion on heat fluxes and the transient response of a two-dimensional ocean modelm *J. Phys. Oceanogr., 25,* 2166-2176, 1995.

Huang, R.X., Real freshwater flux as a natural boundary condition for the salinity balance and thermohaline circulation forced by evaporation and precipitation, *J. Phys. Oceanogr., 23,* 2428-2446, 1993.

Jenkins, A., A one-dimensional model of ice shelf-ocean interaction, *J. Geophys. Res., 96,* 20671-20677, 1991.

Jenkins, A., and C.S.M. Doake, Ice-ocean interaction on Ronne Ice Shelf, Antarctica, *J. Geophys. Res., 96,* 791-813, 1991.

Killworth, P.D., A two-dimensional model for the formation of Antarctic Bottom Water, *Deep Sea Res., 20,* 941-971, 1973.

Killworth, P.D., Mixing on the Weddell Sea continental slope, *Deep Sea Res., 24,* 427-448, 1977.

Killworth, P.D., On "chimney" formations in the ocean, *J. Phys. Oceanogr., 9,* 531-554, 1979.

Manabe, S., and R.J. Stouffer, Simulation of abrupt climate change induced by freshwater input to the North Atlantic Ocean, *Nature, 378,* 165-167, 1995.

Marotzke, J., Influence of convective adjustment on the stability of the thermohaline circulation, *J. Phys. Oceanogr., 21,* 903-907, 1991.

McCartney, M.S., and L.D. Talley, Warm-to-cold water conversion in the northern North Atlantic ocean, *J. Phys. Oceanogr., 14,* 922-935, 1984.

Moore, A.M., and C.J.C. Reason, The response of a global ocean general circulation model to climatological surface boundary conditions for temperature and salinity, *J. Phys. Oceanogr., 23,* 300-328, 1993.

Semtner, A.J., A model for the thermodynamic growth of sea ice in numerical investigations of climate, *J. Phys. Oceanogro., 6,* 379-389, 1976.

Smith, P.C., A streamtube model for bottom boundary current in the ocean, *Deep Sea Res., 22,* 853-873, 1975.

Strass, V.H., E. Fahrbach, U. Schauer, and L. Sellmann, Formation of Denmark Strait overflow water by mixing in the East Greenland Current, *J. Geophys. Res., 98,* 6907-6919, 1993.

Swift, J.H., The circulation of the Denmark Strait and Iceland-Scotland overflow waters in the North Atlantic, *Deep-Sea Res., Part A, 31,* 1339-1355, 1984.

Swift, J.H., K. Aagaard, and S.-A. Malmberg, The contribution of the Denmark Strait overflow to the deep North Atlantic, *Deep-Sea Res., Part A, 27A,* 29-42, 1980.

Toggweiler, J.R., and B. Samuels, Effect of sea ice on the salinity of Antarctic Bottom waters, *J. Phys. Oceanogr., 9,* 1980-1997, 1995.

Trowbridge, J.H., and S.J. Lentz, Asymmetric behavior of an oceanic boundary layer above a sloping bottom, *J. Phys. Oceanogr., 21,* 1171-1185, 1991.

Wright, D.G., and T.F. Stocker, A zonally averaged ocean model for the thermohaline circulation, I, Model development and flow dynamics, *J. Phys. Oceanogr., 21,* 1713-1724, 1991.

Wright, D.G., and T.F. Stocker, Sensitivities of a zonally averaged global ocean circulation model, *J. Geophys. Res., 97,* 12,707-12,730, 1992.

L.D.D. Harvey, Department of Geography, University of Toronto, 100 St. George St., Toronto, Ontario, Canada M5S 3G3. (email:harvey@geog.utoronto.ca)

(Received December 19, 1994; revised March 15, 1996; accepted March 25, 1996.)